Three-dimensional Analysis of Fatigue Crack Propagation using X-Ray Tomography, Digital Volume Correlation and Extended Finite Element Simulations

Julien Réthoré, N. Limodin, Jean-Yves Buffiere, Stéphane Roux, François Hild

Available online at www.sciencedirect.com

SciVerse ScienceDirect

Procedia IUTAM 4 (2012) 151 – 158

Procedia IUTAM

www.elsevier.com/locate/procedia

Full field measurements and identification in Solid Mechanics

Three-dimensional analysis of fatigue crack propagation using X-Ray tomography, digital volume correlation and extended finite element simulations

Julien Réthoré[a]*, Nathalie Limodin[b], Jean-Yves Buffière[c], Stéphane Roux[d], François Hild[d]

[a] *LaMCoS, INSA Lyon / Université de Lyon / CNRS, F-69621 Villeurbanne Cedex, France*
[b] *LML, Ecole Centrale Lille / CNRS, F-59655 Villeneuve d'Ascq Cedex, France*
[c] *MATEIS, INSA Lyon / Université de Lyon / CNRS, F-69621 Villeurbanne Cedex, France*
[d] *LMT-Cachan, ENS Cachan / CNRS / UPMC / UniverSud Paris, F-94235 Cachan Cedex, France*

Abstract

Fatigue crack propagation is usually analyzed as a one-dimensional problem and the identification of Paris' type propagation law is often performed using standardized samples. The present paper is devoted to the analysis of three dimensional fatigue crack propagation using advanced experimental, imaging, measurement and numerical simulation techniques. Fatigue experiments are performed in situ in a tomograph. The images are analyzed using digital volume correlation to extract displacement fields and crack geometry. Stress intensity factors are evaluated along three-dimensional crack fronts and compared to numerical simulations using measured boundary conditions and detected crack shape. Last, *using a single experiment,* local da/dN vs. ΔK laws are estimated within a large range of ΔK values.

Keywords: digital volume correlation; X-FEM; crack propagation; x-ray tomography.

1. Introduction

Since the work of Paris and Erdogan [1], the most generally accepted formalism for describing the growth of fatigue cracks is the so called (empirical) Paris' law that relates the Fatigue Crack Growth Rate

* Corresponding author. Tel.: +33-4-72-43-87-87; fax: +33-4-72-43-85-78.
E-mail address: julien.rethore@insa-lyon.fr.

 doi:10.1016/j.piutam.2012.05.017

(FCGR) per cycle (da / dN) to the stress intensity factor range (ΔK). While many, more or less sophisticated, methods have been used to obtain experimental values of da / dN in cyclically loaded samples or components (see for example a review in [2] or [3]), the number of experimental methods giving access to ΔK has remained very limited, especially in optically opaque materials such as metals and alloys. This is because any experimental method aiming at "measuring" ΔK should in principle probe the strain field in the vicinity of the crack tip.

In the last decade however, important progress has been made in this field. Three different families of techniques have been used, namely, synchrotron X-ray diffraction strain mapping, displacement field measurement either by Digital Volume Correlation (DVC) or tracking of individual markers and numerical simulation technique dedicated to three-dimensional crack propagation. In some cases, the tomography images are used to evaluate 3D displacement fields near the crack tip in a specimen under load. Toda et al. [4; 5] used tracking of microstructural features, i.e., porosities, inside an Al alloy to map the 3D displacement field close to the crack tip in high resolution tomographic images obtained with a synchrotron source. Digital Volume Correlation (DVC) was also used to extract the Crack Opening Displacement (COD) maps in the cross-section of a pre-cracked specimen [6] while the analysis of the measured 3D displacement field allowed for the SIFs to be computed [7]. It is to be emphasized that DVC, like the microstructural tracking method, can only be applied to materials with a suitable texture, i.e., materials that contain natural markers. Contrary to the 2D case, no "speckle pattern" can be introduced in the specimen except by adding artificial markers at the material processing step [8] but then the risk to affect the material properties is high. Further, discretization strategies dedicated to cracks such as the eXtended Finite Element Method (X-FEM) now allow the presence of a crack of arbitrary geometry to be accounted for in an existing FE model without modifying the mesh [9]. X-FEM has recently been used in order to measure discontinuous displacement fields in 2D using X-DIC [10] but also in 3D using X-DVC [6]. This approach combines experiments, measurements and numerical simulations of 3D fatigue crack propagation in a seamless way.

2. Experimental setup

To obtain small fatigue pre-cracked specimens, notched specimens with a $6 \times 4\ mm^2$ cross-section were machined from a heat treated cast iron bar and loaded in fatigue at room temperature (load ratio = 0.1; frequency = 10 Hz). The specimen faces were mirror polished prior to the fatigue experiment to allow for crack growth detection and monitoring with a travelling optical microscope. A load-shedding technique was used to maintain the maximum Stress Intensity Factor (SIF) K_{max} less than 12.8 MPa$\sqrt{m}$ so that confined plasticity prevails at the crack tip with a plastic zone size (in plane strain) smaller than 170 µm. Fatigue cycling was stopped when the observed crack was 1.5-mm long. For the tomography experiment, two smaller specimens with a $1.6 \times 1.6\ mm^2$ cross-section were spark cut inside the large samples. One sample was cut from one side of a large pre-cracked specimen so that the crack tip experienced plane stress to plane strain conditions during fatigue pre-cracking. The tomography experiment was performed on ID19 beamline at the European Synchrotron Radiation Facility (ESRF) in Grenoble, France. A monochromatic X-Ray beam ($\Delta\lambda / \lambda = 10^{-2}$) having a photon energy of 60 keV traverses the sample giving an incident-to-transmitted intensity ratio of about 10%. A Fast Readout Low Noise (FReLoN) 14-bit CCD camera with a 2048×2048 pixel sensor was utilized. A specially designed fatigue machine allowing for in-situ loading and high frequency cycling (up to 50 Hz) of the specimens was used [11]. A PMMA tube, almost transparent to X-rays, was chosen as loading rig. The machine was directly mounted on the rotating stage of the beam line. To obtain a complete scan of the specimen cross-section in the vicinity of the crack, six hundred radiographs were taken while the sample was rotating over 180 ° along its vertical axis; acquisition of a complete scan lasted about 45 minutes. Reconstruction of the

tomographic data was performed with a standard filtered back-projection algorithm [12]. It provides a 3D image with a grayscale color map that is proportional to the local X-ray attenuation coefficient. Although better resolutions are achievable, a 5.06-µm voxel size was chosen as a compromise between the image texture and the size of the reconstructed 3D images obtained from tomography. It is much smaller than the graphite nodule average size in order to allow for good quality images to be obtained while it is also large enough for the size of the region of interest, which was focused around the crack, to be only $340 \times 340 \times 512$ voxels in size. This limited data size enabled for the DVC measurements to be performed on line during the tomography experiment (i.e., the computation time is less than the scan time on a PC with quad-core processor, and of the same order as the reconstruction duration). The cast iron with spherical graphite nodules was chosen for this experiment as its fatigue crack growth behavior has been extensively studied [13] and as the contrast between the ferritic matrix and the graphite nodule provides images that are quasi ideal for DVC. Nodules are about 50 µm in diameter (about 10 voxels) and their volume fraction is estimated to be of the order of 14%. However the DVC algorithm used herein has also been tested on materials that provide much less ideal images such as polypropylene foam [14], stone wool [15] or gray (lamellar graphite) cast iron.

In order to obtain 3D pictures of the specimen during the initial loading cycle, and thereafter for different stages of cyclic loading, the specimen was first gradually loaded up to a maximum level, which is expected to result in a K_{max} value slightly less than that used for fatigue pre-cracking with a mean level that is adjusted to obtain a 0.1-load ratio during cycling under constant amplitude. At the beginning of the experiments, scans were acquired at intermediate loading steps from the maximum to the minimum load level of the first unloading / loading cycle. Then during the in-situ fatigue experiment, scans were recorded at different time intervals with the specimen held under maximum load. When crack growth was detected in these images, e.g. after (n-1) cycles, another complete loading / unloading sequence was recorded at the n^{th} cycle. The fatigue experiment was conducted until the unbroken ligament became too short for further crack propagation. Figure 1 shows two reconstructed tomographic images of the sample. The first image corresponds to the unloaded state prior to any fatigue cycle and the second one to the maximum load after 45,000 fatigue cycles.

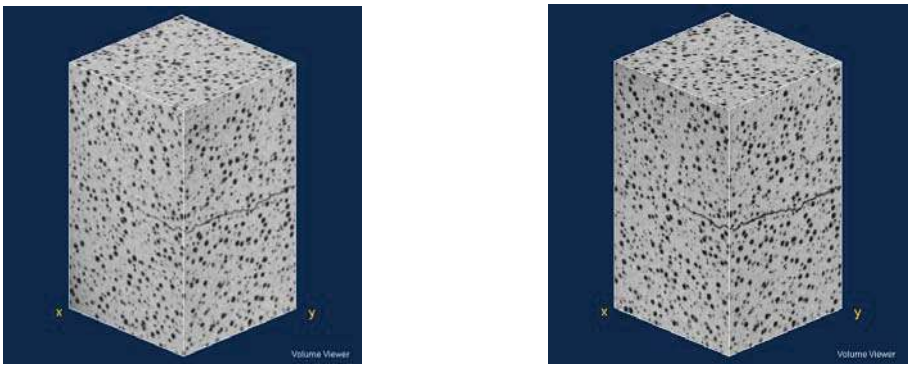

Fig. 1. X-ray tomography images (left: at zero load for the 1st cycle; right: at maximum load after 45,000 fatigue cycles) of the nodular graphite cast iron specimen with a fatigue pre-crack.

3. Digital Volume Correlation (DVC)

Digital Volume Correlation (DVC) is the three dimensional extension of Digital Image Correlation. The gray level conservation law is applied in 3D, and the 3D displacement field that produces the passive advection of the image texture is searched for

$$f(\boldsymbol{x})=g(\boldsymbol{x}+\boldsymbol{u}(\boldsymbol{x})) \quad (1)$$

where f is the discrete gray-level valued function representing the reference 3D image, g the corresponding discrete function representing the advected image, $\boldsymbol{x}$ the vector that defines the position of any voxel and $\boldsymbol{u}$ the searched displacement. Once a basis has been chosen to decompose the displacement field, a non-linear least-squares resolution of this equation is adopted. To combine measurements and numerical simulations, the displacement field is decomposed over a finite element basis function defined on a regular mesh of hexahedra. After the displacement field has been calculated, the quality of the computed solution is controlled, namely, $|f(\boldsymbol{x})-g(\boldsymbol{x}+\boldsymbol{u}(\boldsymbol{x}))|$ is the appropriate error indicator for such DVC displacement measurements. This is referred to as residual map hereafter. Figure 2 shows the displacement measured in the loading direction between the reference volume and the deformed volume shown in Figure 1. The displacement is expressed in voxels (1 voxel being 5.06 μm). An abrupt variation of the displacement is observed through the mid-plane of the studied region. The latter covers a region of 320 × 288 × 288 voxels approximately centered about the mean crack plane in the loading direction (X). The mesh consists in 8-noded cube elements of 32 voxels with a tri-linear interpolation (it will be referred to as C8-DVC). The displacement amplitude is about 3 voxels once rigid body motions (translation and rotation) have been subtracted from the whole displacement. In Figure 2 the corresponding residual map is also depicted. The residual in gray level has been normalized by the dynamic range of the image and is expressed in percent. High residual levels (up to 20% of the dynamic range) are localized on the crack surface that can be clearly distinguished from the microstructure of the material. Elsewhere, the mean residual level is about 5%, which means that the image texture is properly advected by the computed displacement field. Moreover, the original image texture cannot be distinguished in the residual field. It appears to be close to the white noise texture expected for a successful image registration.

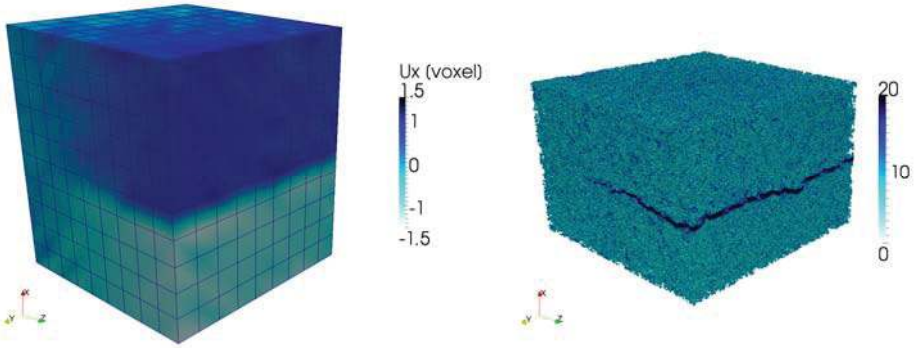

Fig. 2. Vertical displacement field obtained by using a C8-DVC analysis (left). Corresponding correlation residual map expressed in percent of the image dynamic range (right).

4. Crack detection and eXtended DVC

From this residual map, a dedicated shape detection algorithm is developed to capture the crack geometry [16]. The crack surface is described implicitly by a level set. A signed distance function is built, whose iso-0 surface describes the crack. This surface is moved so that it runs through the voxels with maximum residual level. Figure 3 shows the thresholded error map and how the detected surface fits the set of voxels with the highest residual levels.

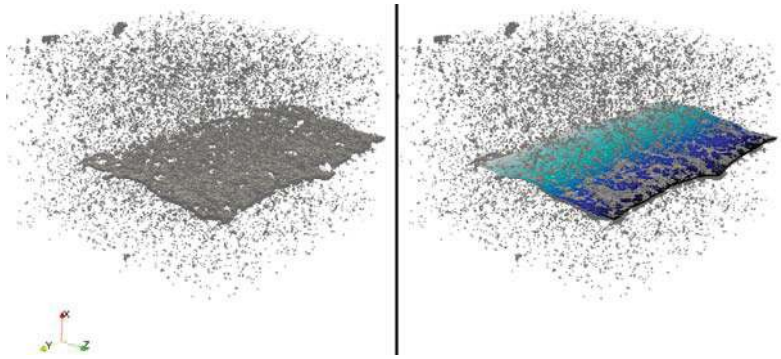

Fig. 3. Thresholded error map (left) and the detected crack surface (right).

After the crack surface is obtained, the displacement approximation is enriched with discontinuous functions in the framework of X-FEM. It allows accounting for discontinuities without requiring an explicit mesh of their geometrical support. The displacement approximation is thus decomposed in a standard contribution, which is based on classical finite element, and an enriched part that contains discontinuous functions across the crack surface. Compared to classical C8-DVC, the mesh remains unchanged but the displacement discretization is enriched. Figure 4 shows the displacement along the loading direction that was obtained when using such enrichments based on the crack surface depicted in Figure 3. The discontinuity is now accounted for in the displacement field, and a crack opening displacement map can be plotted as shown in Figure 5. The latter shows the displacement discontinuity expressed in voxel along the loading direction (i.e., mode I) plotted on the detected crack surface.

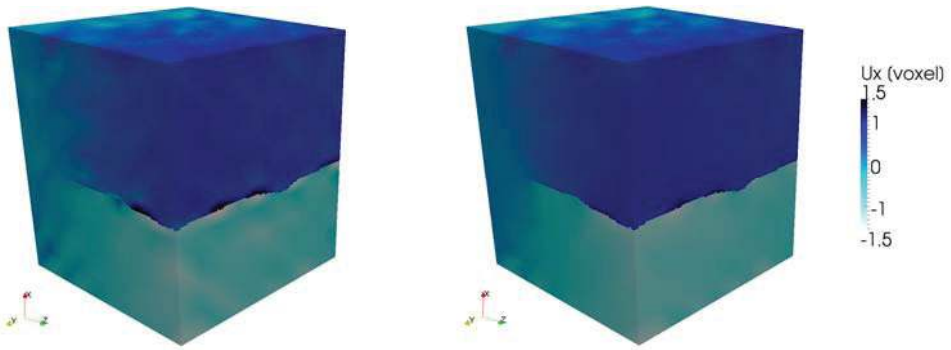

Fig. 4. Vertical displacement field in voxel obtained using an eXtended Finite Element DVC analysis (left) and from a numerical simulation using DVC displacement on the top and bottom surface of the mesh as boundary conditions (right).

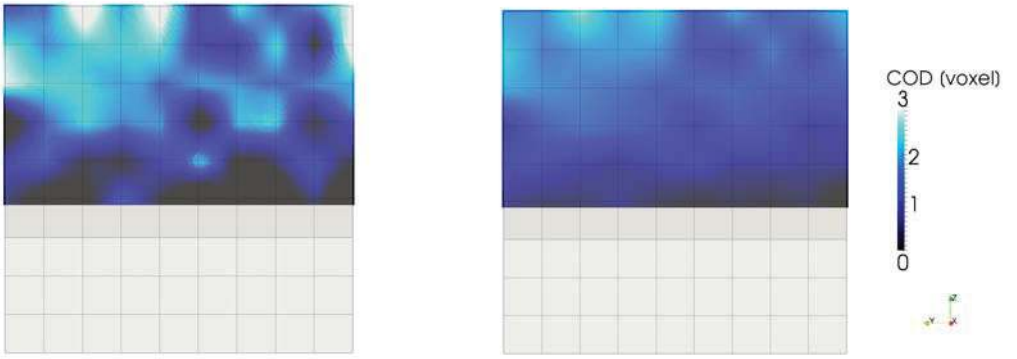

Fig. 5. Mode I opening displacement field (in voxels) obtained when using an XC8-DVC analysis (left) and from a numerical simulation using DVC displacements on the top and bottom surface of the mesh as boundary conditions (right).

5. X-FEM simulations and stress intensity factors

The displacement on the bottom and top faces of the mesh obtained from an X-DVC analysis are used as boundary conditions for a linear elastic simulation. In Figures 4 and 5 the measured results (with XC8-DVC) are compared with X-FEM simulations in terms of displacement field and displacement jump field along the loading direction. A good agreement is obtained. Further, the stress intensity factors are extracted along the crack front for both measured and simulated displacement fields. Figure 6 shows the comparison of mode I, II, and III stress intensity factors for the two analyses [7]. Again, a quantitative agreement is obtained. However the simulated results are smoother since the only uncertainty source in this analysis comes from the noise in the boundary conditions. Its influence vanishes rapidly because the displacement field is obtained from a mechanical simulation.

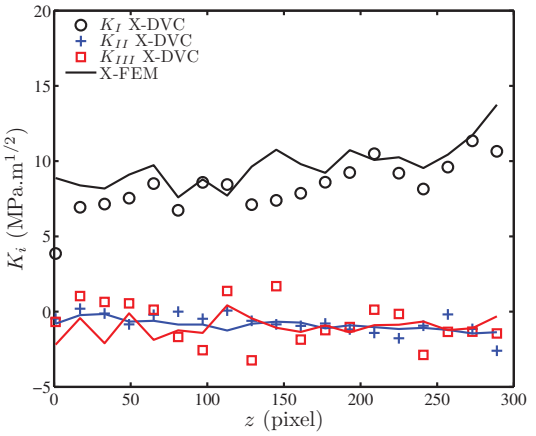

Fig. 6. Comparison of stress intensity factors between X-DVC and numerical simulations (X-FEM) using X-DVC displacements as boundary conditions of X-FEM calculations.

Stress intensity factors and crack tip positions are extracted for all the fatigue cycles for which a tomographic scan was acquired. The crack growth rate is thus estimated and the stress intensity factor range. All these data are plotted in log scale on a single graph in Figure 7. From these data, a local estimate of a modified Paris' law is obtained, namely, a threshold stress intensity factor, which compares well to the value measured by Nadot et al. [17] for a similar material (dashed line in Figure 7). Coefficients in the *da* / *dN* vs. *ΔK* relationship are close, but not identical, to the Paris' law coefficients measured by Dierickx [13] for long cracks in CT specimens of the same material.

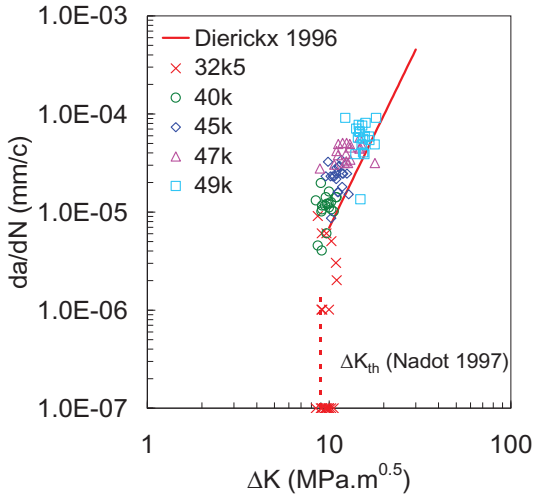

Fig. 7. Fatigue crack growth rate as a function of the stress intensity factor range (*ΔK*). Local estimates of both quantities obtained along the crack front for five scans acquired at different loading cycles are plotted in log / log scale.

6. Conclusion

A methodology is proposed to extract local Paris' law from local estimates of crack growth rate and stress intensity factor range along the front of a three dimensional crack. From reconstructed volumes obtained with computed tomography, digital volume correlation allowed us to measure 3D displacement fields. When post-processing the latter ones, crack front positions were determined and stress intensity factor ranges were evaluated.

Comparison with numerical simulations using the same kinematic description (X-FEM), the same crack geometry, and the measured displacement as boundary conditions demonstrates how crack propagation can be simulated in order to validate the identified parameters.

Acknowledgements

This work was funded by the CETIM Foundation under the grant PROPAVANFIS ('Advanced methods for the experimental and numerical analyses of crack propagations under complex loadings') and by the Agence Nationale de la Recherche under the grant ANR-09-BLAN-0009-01 (RUPXCUBE Project). This work was also made possible by an ESRF grant for the experiment MA-501 on beamline ID19.

References

[1] Paris PC, Erdogan FA. A Critical Analysis of Crack Propagation Laws. *J Bas. Eng. Trans., ASME, Series D* 1963, **85**:528-534.

[2] Hudak SJ, Bucci RJ. Fatigue Crack Growth Measurement and Data Analysis. *ASTM STP738* 1981.

[3] Schijve J. *Fatigue of structures and materials*. Kluwer Academic; 2001.

[4] Toda H, Sinclair I, Buffière JY, Maire E, Connolley T, Joyce M, Khor KH, Gregson P. Assessment of the fatigue crack closure phenomenon in damage-tolerant aluminium alloy by in-situ high-resolution synchrotron X-ray microtomography. *Phil. Mag.* 2003, **83**:2429-2448.

[5] Toda H, Sinclair I, Buffière JY, Maire E, Khor KH, Gregson P, Kobayashi T. A 3D measurement procedure for internal local crack driving forces via synchrotron X-ray microtomography. *Acta Materialia* 2004, **52**:1305-1317.

[6] Réthoré J, Tinnes J, Roux S, Buffière J, Hild F. Extended three-dimensional digital image correlation (X3D-DIC). *CR Mécanique* 2008, **336**:643-649.

[7] Limodin N, Réthoré J, Buffière JY, Gravouil A, Hild F, Roux S. Crack closure and stress intensity factor measurements in nodular graphite cast iron using three-dimensional correlation of laboratory X-ray microtomography images. *Acta Materialia* 2009, **57**:4090-4101.

[8] Nielsen SF, Poulsen HF, Beckmann F, Thorning C, Wert JA. Measurements of plastic displacement gradient components in three dimensions using marker particles and synchrotron X-ray absorption microtomography. *Acta Materialia* 2003, **51**:2407-2415.

[9] Moës N, Gravouil A, Belytschko T. Non-planar 3D crack growth by the extended finite element and levelsets. Part I: Mechanical model. *Int. J. Num. Eng.* 2002, **53**:2549-2568.

[10] Réthoré J, Hild F, Roux S. Extended digital image correlation with crack shape optimization. *Int. J. Num. Eng.* 2007, **73**:248-272.

[11] Buffière JY, Ferrié E, Proudhon H, Ludwig W. Three-dimensional visualisation of fatigue cracks in metals using high resolution synchrotron X-ray micro-tomography. *Mat. Sci. Tech.* 2006, **22**:1019-1024.

[12] Kak AC, Slaney M. *Principles of Computerized Tomographic Imaging*. Society of Industrial and Applied Mathematics; 2001.

[13] Dierickx P. *Etude de la microstructure et des mécanismes d'endommagement de fontes G.S. ductiles : influence des traitements thermiques de ferritisation* (in French). PhD thesis. INSA de Lyon, 1996.

[14] Roux S, Hild F, Viot P and Bernard D. Three-dimensional image correlation from X-ray computed tomography of solid foam. *Comp.*:Part A. 2008, **39**: 1253-1265.

[15] Hild F, Maire E, Roux S and Witz JF. Three-dimensional image analysis of a compression test on a stone wool. *Acta Materialia*. 2009, **57**: 3310-3320.

[16] Rannou J, Limodin N, Réthoré J, Gravouil A, Ludwig W, Baietto-Dubourg MC, Buffière JY, Combescure A, Hild F, Roux S. Three dimensional experimental and numerical analysis of a fatigue crack. Comp. Meth. App. Mech. Eng. 2009, **99**:1307-1325.

[17] Nadot Y, Ranganathan N, Mendez J, Béranger AS: Study of natural cracks initiated on casting defects by crack front marking. *Scripta Materialia* 1997, **37**:549-553.